Effect of long-term irrigation and tillage practices on X-ray CT and gas transport derived pore-network characteristics

Müller, Karin; Dal Ferro, Nicola; Katuwal, Sheela; Tregurtha, Craig; Zanini, Filippo; Carmignato, Simone; Wollesen De Jonge, Lis; Moldrup, Per; Morari, Francesco

Published in:
Soil Research

DOI (link to publication from Publisher):
10.1071/SR18210

Publication date:
2018

Document Version
Accepted author manuscript, peer reviewed version

CSIRO PUBLISHING
Soil Research
https://doi.org/10.1071/SR18210

Effect of long-term irrigation and tillage practices on X-ray CT and gas transport derived pore-network characteristics

Karin Müller[A], *Nicola Dal Ferro*[B,G], *Sheela Katuwal*[C], *Craig Tregurtha*[D], *Filippo Zanini*[E], *Simone Carmignato*[E], *Lis Wollesen de Jonge*[C], *Per Moldrup*[F], *and Francesco Morari*[B]

[A]Plant & Food Research, Production Footprints, Bisley Road, Hamilton 3214, New Zealand.
[B]Department of Agronomy, Food, Natural Resources, Animals and Environment, Agripolis, University of Padova, Viale Dell'Università 16, 35020 Legnaro, Italy.
[C]Department of Agroecology Aarhus University, Blichers Allé 20, PO Box 50, DK-8830 Tjele, Denmark.
[D]Plant & Food Research, Soil Water and Environment, Gerald Street, Lincoln 7608, New Zealand.
[E]Department of Management and Engineering, University of Padova, Stradella San Nicola 3, 36100 Vicenza, Italy.
[F]Department of Civil Engineering, Aalborg University, Thomas Manns Vej 23, Aalborg Ø, 9200-Denmark.
[G]Corresponding author. Email: nicola.dalferro@unipd.it

Abstract. The gas transport parameters, diffusivity and air-filled porosity are crucial for soil aeration, microbial activity and greenhouse gas emission, and directly depend on soil structure. In this study, we analysed the effect of long-term tillage and irrigation practices on the surface structure of an arable soil in New Zealand. Our hypothesis was that topsoil structure would change under intensification of arable production, affecting gas exchange. Intact soil cores were collected from plots under intensive tillage (IT) and direct drill (DD), irrigated or rainfed. In total, 32 cores were scanned by X-ray computed tomography (CT) to derive the pore network >30 μm. The cores were then used to measure soil-gas diffusivity, air-permeability and air-filled porosity of pores close to the resolution of the X-ray CT scans, namely ≥30 μm. The gas measurements allow the calculation of pore-network connectivity and tortuosity parameters, which were compared with the CT-derived structural characteristics. Long-term irrigation had little effect on any of the parameters analysed. Total porosity tended to be lower under IT than DD, whereas the CT-derived porosity was comparable. Both the CT-derived mean pore diameter (MPD) and other morphological parameters, as well as gas measurement-derived parameters, highlighted a less developed structure under IT. The differences in the functional pore-network structure were attributed to SOC depletion and the mechanical disturbance through IT. Significant correlations between CT-derived parameters and functional gas transport parameters such as tortuosity and MPD were found, which suggest that X-ray CT could be useful in the prediction of gas transport.

Additional keywords: carbon depletion, Dexter index, intensive tillage, *P*-parameter, soil organic carbon, soil structure.

Received 22 July 2018, accepted 19 September 2018, published online 16 November 2018

Introduction

Modern agriculture associated with increased inputs of agrichemicals, irrigation and intensive cultivation has led to soil compaction and erosion, which negatively affect the delivery of soil ecosystem services. Concomitant are environmental problems such as enhanced greenhouse gas emissions, and degradation of soil and water quality. Soil degradation manifests itself in reduced soil organic matter contents and loss of soil structure, and is threatening the resilience and productivity of agricultural soils.

It is commonly accepted that intensive tillage (IT) results in losses of soil organic carbon (SOC), decreased aggregate stability, and lessivage of finer particles leading to the degradation of soil structure (Pagliai *et al*. 2004; Puget and Lal 2005). In line with this, many studies have shown that reduced tillage can change physical and chemical soil properties and can confine the environmental effects of IT (Dick 1983; Tebrügge and Düring 1999; Pagliai *et al*. 2004; D'Haene *et al*. 2008; Vogeler *et al*. 2009; Ludwig *et al*. 2011; González-Sánchez *et al*. 2012).

Irrigation is a key management practice of modern agriculture and is indispensable for today's food security, especially in the face of climate change. In fact, globally at least 33% of today's food is produced under irrigation (Siebert and Döll 2010). Less is known about the long-term influence of irrigation practices on soil properties. Recently, Trost *et al*. (2013) reviewed 14 long-term studies investigating the effect of irrigation on SOC under arable production and concluded

that the direction of change in SOC stocks was mainly dependent on the climate and the initial carbon content of soil. The additional water input increases soil moisture, which enhances plant growth, leading to higher input of organic carbon. However, it also promotes soil microbiological activities, which enhance microbial decomposition of organic matter. It is not trivial to predict how irrigation will affect SOC content, which is intrinsically linked to soil structure. Even less is known about the interactions between long-term irrigation and tillage practices and their combined effect on SOC and architecture. Recent research by Pareja-Sánchez *et al*. (2017) highlighted that irrigation has led to greater susceptibility to topsoil structural degradation, which in turn was mitigated by adopting conservation tillage practices.

Understanding of the gaseous flow through soils and soil-air exchange with the atmosphere is required for understanding many soil functions including carbon sequestration and the related emission of greenhouse gases (Ball 2013). Gas transport in soil is dependent on the pore-network characterised by its pore size distribution, connectivity, tortuosity and water content, and as such, is influenced by soil management including tillage and irrigation. Accurate prediction of air permeability and gas diffusivity requires quantifying parameters describing the pore-network, in particular, tortuosity and connectivity (Ball 1981*a*). Previous studies have used non-invasive imaging techniques including X-ray computed tomography (CT) to analyse the effect of management practices on soil structure (Papadopoulos *et al*. 2009; Schlüter *et al*. 2011; Garbout *et al*. 2013; Munkholm *et al*. 2013; Dal Ferro *et al*. 2014; Piccoli *et al*. 2017*a*). Few studies have linked CT-derived morphometrical parameters to functional parameters derived from gas flow measurements (Naveed *et al*. 2013; Katuwal *et al*. 2015). Our hypothesis is that structural characteristics including pore size distribution, connectivity and tortuosity of surface soil will change under long-term intensive arable production and that these changes can compromise some pivotal soil functions, such as soil-air gas flow and exchange.

Our main objective was therefore to assess the potential effect of long-term irrigation and IT practices on soil quality and pore network in a representative arable soil in the South Island of New Zealand. We analysed the pore-network architecture of a topsoil that had been 14 years under different management practices using X-ray CT, air permeability and gas diffusion measurements. Our specific aim was to identify structure-related soil parameters that may be used as proxies to quantify soil physical quality and its functionality.

Materials and methods

Site description

The study site (−43.79°N, 171.96°E, altitude 109 m) is located on a research farm of the Foundation for Arable Research (FAR) in Chertsey, Canterbury, New Zealand. The warm, temperate climate is characterised by long-term average annual rainfall of 699 mm and annual temperature of 11.2°C. Rainfall is evenly distributed throughout the year with a difference of ~20 mm between the driest and the wettest month. The shallow silt loam soil is classified as Pallic Soil (Hewitt 2010), which corresponds to a Cambisol (FAO 2006).

The long-term cultivation and irrigation experiment was established in 2003. The crop rotation at the site is typical for the Canterbury region involving wheat (*Triticum aestivum* L.), peas (*Pisum sativum* L.), ryegrass (*Lolium perenne* L.) and linseed (*Linum usitatissimum* L.). At the time of the soil sampling for this study, the soil was under the second year of ryegrass grown for seed. The experimental design is a split-plot experiment with irrigation as main plot established in duplicate and cultivation as split plots (25 m × 12 m). The treatments are a combination of two irrigation practices (non-irrigated and irrigated with a lateral travel spray irrigator to a non-stress situation for the respective crop) on the four main plots with six cultivation practices allocated randomly to each of the main plots. We only included the two most extreme cultivation management practices in this study. These were the IT treatment, which includes 20–25 cm depth ploughing, followed by two passes of a Vaderstad Topdown cultivator and John Deere 750A double disc drill, and the direct drill (DD) practice using a cross-slot drill. No organic amendments were applied. The site is under conventional management.

Soil sampling

Soil samples were collected from four randomly selected locations in each split plot at a depth of 0–5 cm in April 2017. At each location a disturbed bulk sample, an undisturbed soil core (5 cm I.D. × 5 cm length) and another intact core (6 cm I.D. × 3 cm length) were taken. Soil cores were excavated by slowly pushing PVC cylinders into the soil. The soil samples were kept cool until delivery to the laboratory. All soil cores were then immediately placed into a hot water bath (0.5 cm water depth) for three hours to dispel earthworms from the cores. All samples were stored at 4°C until further analysis.

Chemical analysis

The disturbed samples were sieved to <2 mm. Total SOC content was determined on 0.5–1.0 g sub-samples by an automated dry combustion method (Dumas) using a LECO TruMac CN analyser (Leco Corporation, MI, USA) operating at 1250°C (Blakemore *et al*. 1987). Hot-water extractable carbon (HWC) was determined using the method developed by Ghani *et al*. (2003). Dissolved organic carbon in the HWC extracts was determined by high-temperature catalytic combustion using a Shimadzu TOC-V CSH total organic carbon analyser.

X-ray computed tomography, image processing and analysis

The intact soil cores (5 cm I.D. × 5 cm length) were air-dried for about a week before trimming their surfaces to exact size. Then, they were saturated from the bottom and equilibrated on pressure plates to a matric potential of −150 cm to ensure uniform conditions before X-ray CT scanning. Each entire soil core was scanned using a metrological X-ray CT system MCT225 (Nikon Metrology, Tring, UK). A metrological X-ray CT system was used to obtain more accurate dimensional measurements (Khademzadeh *et al*. 2016; Zanini and Carmignato 2017). The source was set to 210 kV and 167 µA. A 0.1-mm copper filter was used to minimise beam-

hardening effects. The software Inspect-X Vers. XT 3.1.9 provided by Nikon Metrology was used for the acquisition of bi-dimensional projections. The resulting 1500 2D-projection images (resolution of 33 µm) at 16-bit depth were filtered with a 3×3 median filter to reduce noise and reconstructed using the software CT PRO 3D Vers. XT 3.1.9, provided by Nikon Metrology. The reconstructed volumes where aligned using the analysis and visualisation software VGStudio MAX 3.1 (Volume Graphics GmbH, Heidelberg, Germany) so that the vertical axis coincided with the axis of the external PVC cylinder. Cross-sectional 2D images of the reconstructed volume were segmented into binary images (i.e. soil pores and matrix) using the machine learning-based approach Waikato Environment for Knowledge Analysis (Weka) implemented in ImageJ (Arganda-Carreras *et al*. 2017). This plugin uses a pixel classification system in which each pixel is classified as belonging to a specific class by leveraging the users' identification of object features within a set of images. Finally, the system applies the classification to the image stack, creating a fully segmented dataset. After binarisation, a cylindrical region of interest, representing the largest volume fully occupied by soil, was manually selected for each image stack excluding the PVC cylinder. At least 1400 continuous slices per soil sample were selected. Total porosity detected by CT (TP_{CT}) was calculated by dividing the number of pore voxels by the total number of voxels per core volume. The pore size distribution was obtained as an average of the local thickness of every voxel representing pores (Ulrich *et al*. 1999). The output of the calculation is a histogram with an interval of two pixels. To facilitate the comparison of the pore size distribution, we grouped pores into the following five arbitrarily chosen classes: 33–300, 300–700, 700–1003, 1003–3000 and >3000 µm. In addition, a set of X-ray CT-derived structural parameters were quantified: the degree of anisotropy (DA), as an indicator of the 3D pore symmetry-asymmetry (range from 0 to 1; Harrigan and Mann 1984); the 3D fractal dimension (FD), which describes the self-similarity (scale invariance) of an object, as an indicator of surface complexity (Perret *et al*. 2003); the connectivity density (CE), computed by dividing the connectivity calculated with the Euler-Poincaré equation (Vogel 1997) with the volume analysed; the structure model index (SMI; Hildebrand and Rügsegger 1997), that measures the pore geometry from plate-like (values close of 1) to rod-like shapes (values close to 3, cylinders, or 4, spheres); the object surface-to-volume ratio (OSVR), estimated by dividing the total pore surface by its volume, that characterises the pore structure complexity, thickness and roughness; and the tortuosity (T), determined by relating the sum of the distances of the centroids of the pores between adjacent slices to the height of the image stack (Katuwal *et al*. 2015). Finally, a CT-based tortuosity-connectivity parameter (X_{CCT}) was derived following Katuwal *et al*. (2015).

Gas parameter measurements

The soil cores were drained to –100 cm matric potential before the gas transport measurements. The air-filled porosity (ε_a, $cm^3\ cm^{-3}$) was obtained from the total porosity (TP) and the volumetric water content of the soil at –100 cm matric potential. The air permeability was determined using a laboratory air permeameter, the description and procedure of which are provided in Schjønning and Koppelgaard (2017). Briefly described, the convective air flow rates were measured at four pressure gradients (around 5, 2, 1 and 0.5 hPa). A second-order polynomial equation was fitted between the pressure difference (ΔP) and the air flow velocity (v) as:

$$\frac{\Delta P}{L_s} = a \times v + b \times v^2 \quad (1)$$

where L_s is the sample length (m), and a and b are fitting coefficients. The intrinsic air permeability (k_a, μm^2) was calculated as the ratio of air viscosity (η) and a (Schjønning and Koppelgaard 2017):

$$k_a = \frac{\eta}{a} \quad (2)$$

The relative gas diffusivity (D_p/D_0) was measured using the one-chamber gas diffusion apparatus and O_2 as the diffusing gas as described in Schjønning *et al*. (2013). Briefly, the apparatus consists of measuring chambers with O_2 sensors on the top of each chamber. The soil samples were placed in the airtight chambers with their lower end exposed to the ambient air. N_2 gas was used for flushing the closed chamber above the soil top to remove all O_2. The gradient in O_2 concentration between the top and the bottom of the soil sample allowed O_2 gas to diffuse through the sample into the chamber, the concentration of which was recorded every 2 min. The O_2 diffusion coefficient (D_p) was calculated using the non-steady-state method described by Rolston and Moldrup (2002) as:

$$D_p = -\left(V_c \times \frac{L_s}{A_s}\right)\left[\frac{ln\left(\frac{\Delta C_t}{\Delta C_0}\right)}{t}\right] \quad (3)$$

where ΔC_t and ΔC_0 are the differences in O_2 concentration between the two ends of the sample at time $t = t$ and $t = 0$ respectively, V_c is volume of the diffusion chamber, L_s is the sample length (m) and A_s the cross-sectional area of the soil (m^2). The relative gas diffusivity (D_p/D_0) was obtained after scaling D_p by the diffusion coefficient of O_2 gas in free air ($D_0 = 2.05 \times 10^{-5}\ m^2\ s^{-1}$).

Several studies (e.g. Moldrup *et al*. 2001; Kawamoto *et al*. 2006; Chamindu Deepagoda *et al*. 2012) have shown that ε_a, k_a and D_p/D_0 in combination can be used to fingerprint the soil structure using different parameters as described below. The specific permeability was calculated as the ratio of air permeability and air-filled porosity. Specific gas diffusivity refers to the ratio of relative gas diffusivity and air-filled porosity. The gas diffusion-based tortuosity, τ, was calculated using D_p/D_0 and the air-filled porosity (ε_a) at −100 cm matric potential (Moldrup *et al*. 2001) as:

$$\tau = \sqrt{\frac{\varepsilon_a}{D_p/D_0}} \quad (4)$$

The tortuosity-connectivity parameter (X) was calculated as (Chamindu Deepagoda *et al*. 2012):

$$X = \frac{log(D_p/D_0)}{log(\varepsilon_a)} \quad (5)$$

The functional equivalent pore diameter (d, μm) (Ball 1981*a*), was derived as follows:

$$d = 2\sqrt{\frac{8k_a}{D_p/D_0}} \quad (6)$$

where the higher the value, the more continuous and interconnected the pore network (Kawamoto *et al*. 2006; Katuwal *et al*. 2015).

Air permeability was predicted from measurements of D_p/D_0 (e.g. Moldrup *et al*. 1998):

$$k_a = P \times D_p/D_0 \quad (7)$$

where P (μm^2) is a soil structural parameter that is dependent on the equivalent pore diameter (Katuwal *et al*. 2015). It was obtained as the ratio between air permeability and gas diffusivity. High P-parameter values identify a prevailing pipe-like pore-network with continuous pores enhancing convective gas exchange (Kawamoto *et al*. 2006).

Physical analysis

The soil cores were dried in the oven at 105°C for 48 h to determine the volumetric water content and the bulk density (BD) following Blakemore *et al*. (1987). In addition, a sub-sample of the soil cores was sieved to <2 mm and dispersed in a 2% sodium hexametaphosphate solution for soil textural determination by laser diffractometry using a Malver Mastersizer 2000 (Malvern Instruments, Malvern, UK).

Statistical analysis

To account for the split-plot design of the experiment, data were analysed with ANOVA taking irrigation and cultivation and their interaction as fixed effects. Data of each plot were included in the analysis as a within-subplot factor. Variability associated with the modelled means was provided by the least significant difference (l.s.d.) at the 5% level of significance. Heterogeneity of variance was assessed and data were log-transformed if needed. These statistical analyses were carried out using the statistical package GENSTAT (Version 18.2.0.18409, VSN International Ltd). In addition, Pearson's correlation analysis and multiple regression analysis were performed with Statistica (StatSoft Inc., Tulsa, USA) to estimate linear relationships between the analysed variables.

Results and discussion

General soil properties

The topsoil is classified as a silt loam soil (Verheye and Ameryckx 1984). We found a significant ($P < 0.05$) difference in textural composition between the DD and IT topsoil (Table 1). The higher clay (Fig. 1*a*) and silt contents under IT compared with those under DD might be attributed to mixing of soil from deeper depth with higher clay and silt contents into the topsoil through ploughing. Irrigation tended to decrease SOC concentration (−6%; $P = 0.124$; Fig. 1*b*). Tillage resulted in a significant ($P = 0.01$) reduction of SOC (−19%; Fig. 1*b*). This led to a clay-to-carbon ratio (Dexter index; Dexter 2004) of <10 in the DD topsoil and >10 in the IT soil (Table 1; Fig. 1*c*), suggesting the potential for a more developed soil structure in the DD topsoil. Crop residues and yields have been similar for the different tillage treatments at the experimental site since 2003, the start of the experiment. Irrigation has led to significantly higher annual yields throughout the crop rotation (data not shown). Thus we attribute the observed differences in SOC to the result of physical disturbance that likely produced differences in topsoil temperature and water content, and the related effects on soil microbiological activities (Trost *et al*. 2013). Similar positive effects of reduced tillage practices on SOC stocks in the topsoil have been observed in many other studies (Havlin *et al*. 1990; Soane and Ball 1998; Al-Kaisi *et al*. 2005; Puget and Lal 2005). Some studies cautioned that SOC increases in topsoils related to reducing tillage intensity might be the consequence of redistributing carbon with depth (Baker *et al*. 2007; Powlson *et al*. 2014). This suggests that SOC might be stratified differently between DD and IT, with the latter showing SOC content dilution due to the mixing of topsoil and subsoil layers. In accordance with our findings, irrigation had

Table 1. Long-term tillage and irrigation effects on soil properties of an arable soil under a crop rotation typical for Canterbury, New Zealand. The results presented are the predicted means followed by the 5% least significant difference (l.s.d.) to compare means with different tillage and same irrigation treatments (l.s.d.$_{Till}$), and means with different irrigation treatments (l.s.d.$_{Irr}$). The textural parameters, total porosity and bulk density were determined at intact soil cores of 5 × 5 cm depth, and the remaining parameters at bulked soil samples collected beside the intact cores

DD, Direct drill; IT, Intensive tillage

Treatment	Non-irrigated		Irrigated		l.s.d.$_{0.05}$	
	DD	IT	DD	IT	l.s.d.$_{Till}$	l.s.d.$_{Irr}$
Clay (kg kg^{-1})	0.247	0.278	0.251	0.281	0.025	0.058
Silt (kg kg^{-1})	0.522	0.565	0.509	0.565	0.048	0.031
Sand (kg kg^{-1})	0.231	0.158	0.241	0.154	0.053	0.047
Total carbon (kg kg^{-1})	0.031	0.024	0.028	0.022	0.004	0.003
Dexter index (-)	8.02	11.46	8.54	12.65	1.98	3.20
Hot water carbon (10^{-3} kg kg^{-1})	1.098	0.733	1.077	0.634	0.222	0.158
pH (-)	5.74	5.93	5.85	6.19	0.13	0.08
Bulk density (g cm^{-3})	1.202	1.250	1.214	1.286	0.097	0.209
Total porosity (cm^3 cm^{-3})	0.54	0.53	0.54	0.51	0.036	0.077

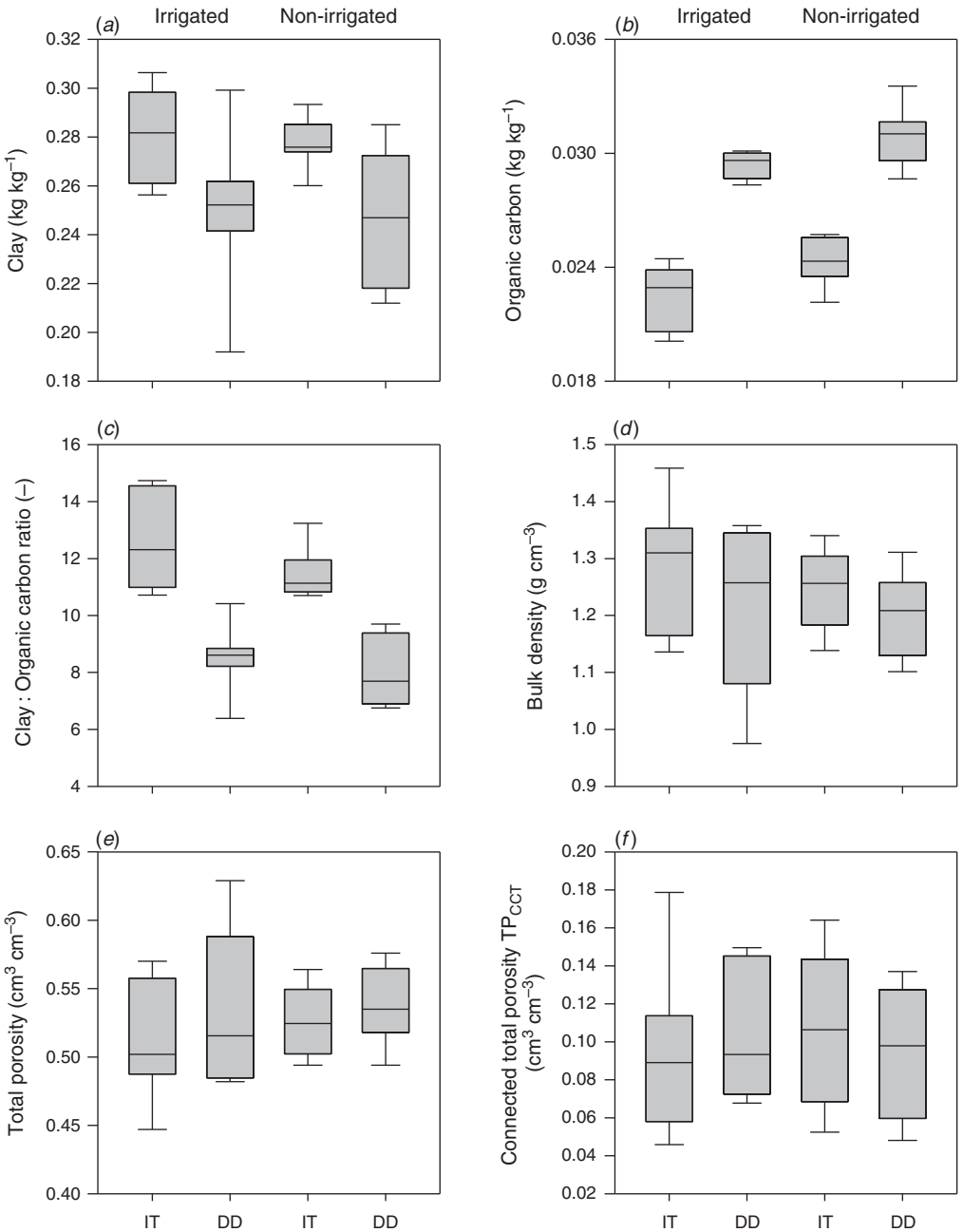

Fig. 1. (*a*) Clay content (kg kg^{-1}), (*b*) soil organic carbon content (kg kg^{-1}), (*c*) clay-to-carbon ratio (Dexter index), (*d*) bulk density (g cm^{-3}), (*e*) total porosity (cm^3 cm^{-3}), and (*f*) connected total porosity detectable in the X-ray CT scans (cm^3 cm^{-3}) of the topsoil (0–5 cm) under different management practices, irrigated and non-irrigated, intensive tillage (IT) and direct drill (DD).

no effect on SOC content in other long-term irrigation studies with arable soils under humid climate. This was explained by high mineralisation (Dersch and Bohm 2001; Trost *et al*. 2013) that likely compensated increased biomass production. Mudge *et al*. (2017) found lower SOC contents under irrigated compared with non-irrigated neighbouring sites with 3 to 33 years of the respective irrigation management history. The authors suggested that a combination of seasonal irrigation in temperate climates and relatively high initial SOC contents were driving factors for decreasing SOC contents. These results support the hypothesis of Trost *et al*. (2013) that the benefits of irrigation to increase SOC contents might be restricted to arid and semiarid ecosystems with low SOC contents. Recently, Chatterjee *et al*. (2018) reported further corroborating findings from a study of the effects of two-year irrigation of maize (*Zea mays* L.) in a semiarid region of India: the initial low SOC content (4.2 g kg^{-1}) significantly increased with irrigation (+40.5%) accompanied by an increase in microbial biomass.

However, few studies have investigated the combined effects of irrigation management and minimum tillage practices. Indeed, some studies found an increase in SOC content (Entry *et al*. 2004), as also found in our study, whereas others (Scott *et al*. 2012) reported decreased SOC driven by reduced crop root growth, which in turn would lower belowground carbon inputs.

The HWC, which is assumed to be closely related to total microbial biomass (Ghani *et al*. 2003), was significantly higher in the DD topsoil than in the IT topsoil (Table 1). This could have been related to the generally lower SOC content in the IT topsoil or to a change in the bioavailability of SOC.

Soil structural parameters

Irrigation had little to no effect on any of the soil physical parameters analysed. Tillage practice led to higher BD ($P = 0.06$; Table 1, Fig. 1*d*) and lower TP ($P = 0.09$; Table 1, Fig. 1*e*) under IT than under DD. SOC was positively correlated with the TP for the IT soil, whereas no such correlation was found for the DD soil (Fig. 2*a*). The lower SOC content of the IT soil was an important factor contributing to the higher BD observed under IT compared with DD (Fig. 2*b*). For the DD soil, BD was more closely related to clay content (Fig. 2*c*). These findings confirm observations made by Dexter *et al*. (2008) working with French and Polish data consisting of arable soils with low carbon contents and pastoral soils with high carbon contents. In other long-term tillage studies, similarly increased topsoil BD under IT has been observed and attributed to stress of heavy machinery on soil structure, which can be exacerbated by high water contents during tillage (Deen and Kataki 2003; D'Haene *et al*. 2008; Badalıkova 2010). However, many studies under temperate climate reported the opposite, increased BD caused by weathering and compaction when leaving soil undisturbed under DD (Yang and Wander 1999; Puget and Lal 2005; Dal Ferro *et al*. 2014; Piccoli *et al*. 2017*b*). Contrasting findings can also be attributed to different lengths of time under each management practice, different soil texture and SOC content.

The same intact soil cores were scanned by X-ray CT to quantify pore-network parameters. Irrigation had no effect on any of these parameters. Nor was the TP detectable by X-ray CT

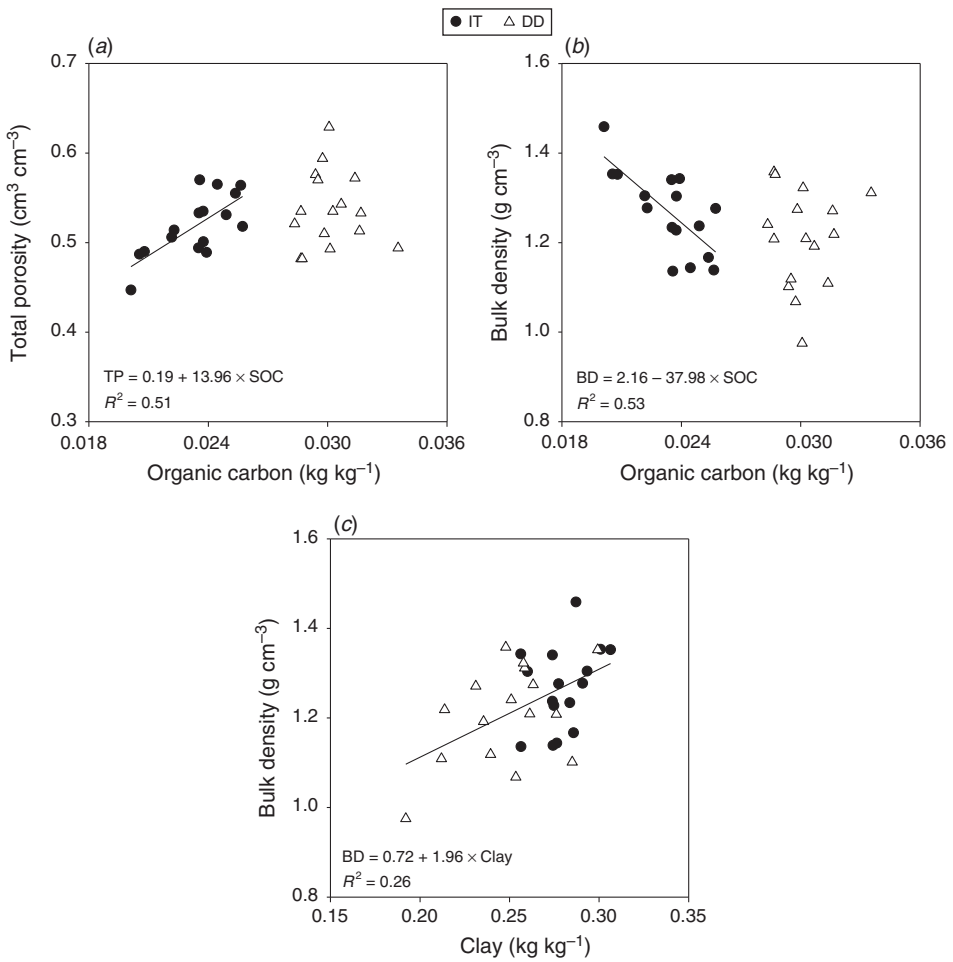

Fig. 2. Relationship between (*a*) total porosity (TP) and total carbon (SOC), (*b*) bulk density (BD) and total carbon (SOC), and (*c*) BD and clay content of the topsoil (0–5 cm) under different management practices, intensive tillage (IT) and direct drill (DD).

($TP_{CT;}$ pores >33 µm) affected by tillage (Fig. 3). The average TP_{CT} was 0.113 cm^3 cm^{-3} and ranged between 12 and 35% of the TP. Limiting the pore volume to the interconnected pore network from the top of a soil core to its bottom ($TP_{CCT;}$ Fig. 1*f*) did not change the results with respect to significance but revealed that a single pore cluster accounted for between 83 and 92% of the TP_{CT} (Table 2). In the following, we only consider this connected porosity TP_{CCT} and its related parameters.

The structural parameters DA_{CCT}, FD_{CCT}, CE_{CCT} and T_{CCT} equally showed a random pattern regardless of management (Table 2). The average degree of anisotropy DA_{CCT} was 0.21, indicating an almost symmetrical structure of the soils. The fractal dimension FD_{CCT} averaged 2.33, the average pore connectivity CE_{CCT}, quantified by the Euler number, was -4.5×10^{-10} μm^{-3}, and tortuosity T_{CCT} was on average 3.2. Although in our study these parameters did not differentiate management practices (Table 2), others reported structural differences due to tillage, for instance, Pagliai *et al*. (2004) found a higher percentage of connected pores under minimum tillage with a disk harrow compared with conventional tillage with mouldboard plough to a depth of 40 cm. In contrast, Pires *et al*. (2017) reported lower connectivity under DD compared with IT.

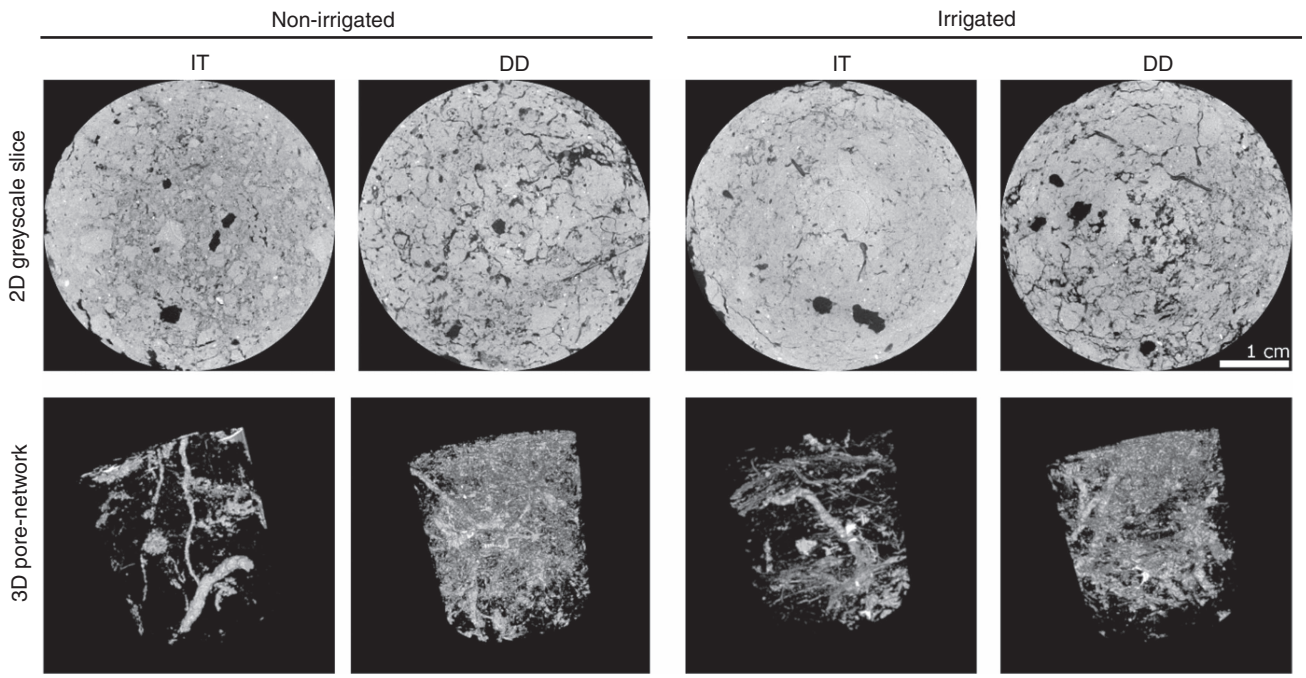

Fig. 3. 2D sections and 3D porosity of selected topsoil cores under long-term tillage (IT, intensive tillage; DD, direct drill) and irrigation practices analysed in this study.

Table 2. Long-term tillage and irrigation effects on soil structural properties of the topsoil (0–5 cm) of an arable soil under a crop rotation typical for Canterbury, New Zealand. All properties were calculated for the CT-visible pores connected from the top to the bottom of a core. The results presented are the predicted means followed by the 5% least significant difference (l.s.d.) to compare means with different tillage and same irrigation treatments ($l.s.d._{Till}$), and means with different irrigation treatments ($l.s.d._{Irr}$)

DD, Direct drill; IT, Intensive tillage; $TP_{CCT;}$ connected total porosity measured with X-ray CT; DA_{CCT}, degree of anisotropy; CE_{CCT}, connectivity; FD_{CCT}, fractal dimension; $OSVR_{CCT}$, object surface-to-volume-ratio; MPD_{CCT}, mean pore diameter; SMI_{CCT}, structure model index; T_{CCT}, tortuosity

Treatment	Non-irrigated		Irrigated		$l.s.d._{0.05}$	
	DD	IT	DD	IT	$l.s.d._{Till}$	$l.s.d._{Irr}$
TP_{CCT} (cm^3 cm^{-3})	0.094	0.106	0.105	0.094	0.044	0.029
DA_{CCT}	0.21	0.20	0.25	0.17	0.28	0.19
$CE_{CCT} \times 10^{-10}$ (μm^{-3})	−5.62	−3.50	−4.44	−4.48	7.950	5.130
FD_{CCT}	2.36	2.33	2.35	2.30	0.20	0.12
$OSVR_{CCT}$ (μm^{-1})	0.008	0.007	0.007	0.007	0.003	0.002
MPD_{CCT} (µm)	681.46	910.43	858.17	913.18	105.99	83.10
SMI_{CCT}	1.63	2.43	1.68	2.18	2.17	1.40
T_{CCT}	3.33	3.21	3.16	3.19	2.40	1.63

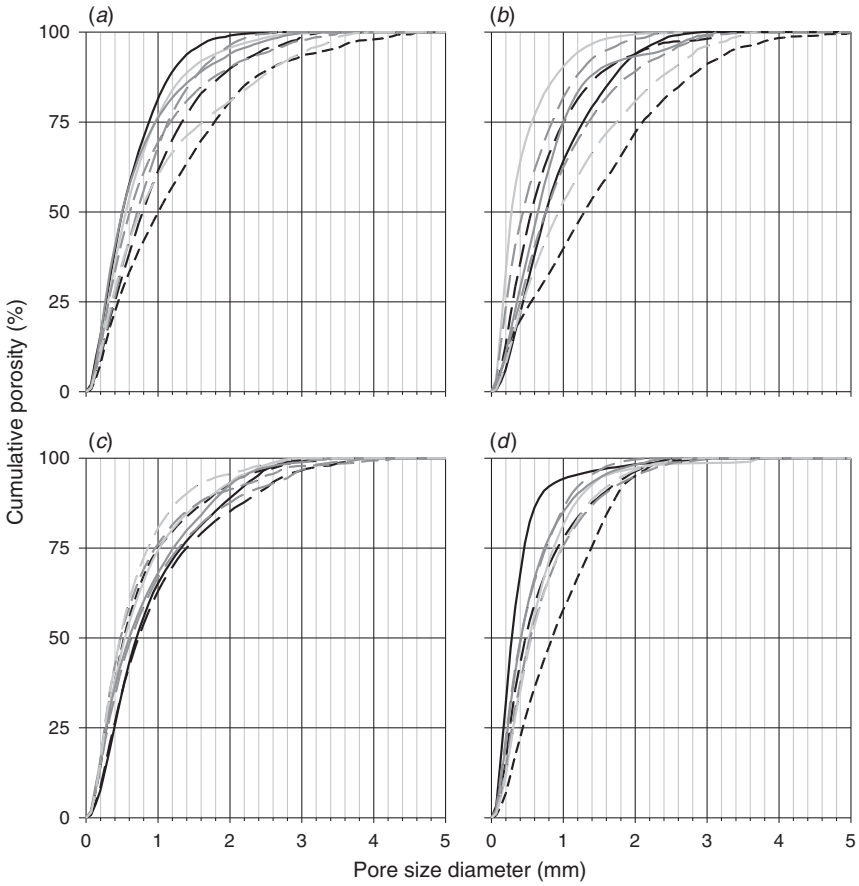

Fig. 4. Pore size distribution of the connected pore volume (TP_{CCT}) for the topsoil (0–5 cm) under (*a*) non-irrigated intensive tillage, (*b*) irrigated intensive tillage, (*c*) irrigated direct drill and (*d*) non-irrigated direct drill determined by X-ray CT. For each treatment eight intact cores were scanned.

Nevertheless, interesting correlations between the CT-derived parameters were found in our study. As suggested by Perret *et al*. (2003), higher values for fractal dimension can describe augmented pore tortuosity or pore complexity. The significant and negative correlation observed between FD_{CCT} and T_{CCT} ($r = -0.6$) highlights that more tortuous pore networks were also dominated by less irregular pore volumes, which did not occupy the entire soil space. Similarly, the correlations between CE_{CCT} and FD_{CCT} ($r = -0.76$) and between CE_{CCT} and T_{CCT} ($r = 0.39$) show that well-connected pore networks were more tortuous, and in turn less scattered throughout the soil matrix. Similar relationships have also been reported in the past for different types of soils, from sandy loam to clay (Chamindu Deepagoda *et al*. 2012; Katuwal *et al*. 2015; Piccoli *et al*. 2017*a*).

Fractal dimension was also correlated strongly and negatively with BD ($r = -0.78$) and positively with sand contents ($r = 0.47$). Usually, FD is found to increase in soils with increasing clay and fine contents (Deng *et al*. 2017). The mechanical effect of regular ploughing overrode this relationship.

In contrast to the above-mentioned structural parameters, IT significantly ($P = 0.005$) increased the mean pore diameter (912 µm) compared with DD (770 µm) (MPD_{CCT}, Table 2).

Table 3. Pore size distribution of the connected pores for the topsoil under long-term irrigation and tillage treatment analysed by X-ray CT. Presented are the predicted mean percentages followed by the 5% least significant difference (l.s.d.) to compare means with different tillage and same irrigation treatments ($l.s.d._{Till}$), and means with different irrigation treatments ($l.s.d._{Irr}$)

DD, Direct drill; IT, Intensive tillage

Treatment	Non-irrigated		Irrigated		l.s.d.	
	DD	IT	DD	IT	$l.s.d._{Till}$	$l.s.d._{Irr}$
30–300 µm	26.63	18.83	21.73	21.62	15.441	10.224
300–700 µm	37.28	32.09	33.98	29.43	3.566	2.075
700–1003 µm	15.29	17.00	15.39	16.52	8.480	5.247
1003–3000 µm	20.59	30.08	27.48	30.56	6.966	4.840
>3000 µm	0.21	2.00	1.43	2.60	4.437	2.585

Object surface-to-volume ratio ($OSVR_{CCT}$) slightly decreased under IT, suggesting that IT augmented both soil disaggregation (Kay and Vanden Bygaart 2002) and pore structure simplification. These results are in agreement with those of soil pore size distribution: indeed, IT showed generally less steep and more variable cumulative porosity curves (Fig. 4*a* and 4*b*) than those of DD (Fig. 4*c* and 4*d*), which were

Table 4. Long-term tillage and irrigation effects on gas parameters of the topsoil (0–5 cm) of an arable soil under a crop rotation typical for Canterbury, New Zealand. Presented are the predicted mean percentages followed by the 5% least significant difference (l.s.d.) to compare means with different tillage and same irrigation treatments (l.s.d.$_{Till}$), and means with different irrigation treatments (l.s.d.$_{Irr}$)

DD, Direct drill; IT, Intensive tillage; τ, tortuosity; X, X-parameter

Treatment	Non-irrigated		Irrigated		l.s.d.	
	DD	IT	DD	IT	l.s.d.$_{Till}$	l.s.d.$_{Irr}$
Air-filled porosity (cm^3 cm^{-3})	0.153	0.161	0.140	0.147	0.080	0.068
Air permeability[A] (μm^2)	114	225	115	222	4.80[B]	5.35[B]
Gas diffusivity	0.033	0.042	0.031	0.042	0.035	0.021
Equiv. pore diameter (μm)	357	482	368	495	401	366
P-parameter	3513	5666	3887	6011	3.69[B]	4.70[B]
τ	2.16	1.99	2.12	1.97	0.46	0.42
X	1.82	1.75	1.76	1.69	0.26	0.41

[A]Removed 2 outliers with large k_a-values due to gap between soil and sleeve during measurements; [B]least-square ratio: smallest ratio for which the ratio between back-transformed means was significant.

also characterised by a larger proportion of smaller pores considering only those detected by X-ray CT (Fig. 3). For all treatments the majority of pores (~70% of TP$_{CCT}$) was smaller than 1003 μm (Table 3). In particular, the absolute volumes of the pore size class 300–700 μm were significantly higher ($P = 0.014$) under DD than under IT. Lower absolute volumes were observed for pores in the size class 1003–3000 μm ($P = 0.032$) for DD compared with IT, leading to larger variability in the pore size distributions and reflecting more disturbed soil conditions with tillage. In contrast, larger pores were often found under DD than under IT due to earthworm activities and root growth (Wahl *et al*. 2004), but results depend on depth, pore size class considered, and soil type. The irrigated topsoil under IT (Fig. 4*b*) had the highest percentage of large pores (>3 mm) as well as the largest pores, albeit these did not contribute more than max 9% to the TP$_{CCT}$, the average contribution was 2.6% (Table 3).

Finally, the structure model index, SMI a measure for the plate- or rod-like geometry of pores (Hildebrand and Rügsegger 1997), likewise was increased ($P = 0.1$), indicating that in the IT soil pores tended to have a cylindrical (SMI = 2.3) rather than plate-like (SMI = 1.65) shape. It must be noted that the X-ray CT analysis was conducted only on pores >33 μm, which contributed ~19% to the TP in our soils, thus limiting the understanding of soil microstructural changes.

Functional structural parameters for gas exchange processes: gas diffusivity and air permeability

The k_a of the topsoil, determined at the same soil cores used for X-ray CT scanning at a matric potential of −100 cm, was classified as 'fast' (101–200 μm^2) to 'very fast' (>201 μm^2) according to Fish and Koppi's (1994) scoring classes. These results suggest that the topsoil had a good structure with many interaggregate pores. Air permeability is the dominant control for air exchange processes in the topsoil. Irrigation treatment had little influence on k_a, whereas tillage increased k_a ($P = 0.15$; Table 4). In a five-year experiment, Piccoli *et al*. (2017*b*) found little to no difference in k_a between tilled and non-tilled silty loam soils, although characterised by lower SOC content (~10 g kg^{-1}) and higher BD (>1.45 g cm^{-3}) compared with the soils used in our study. In contrast, Vogeler *et al*. (2009) found

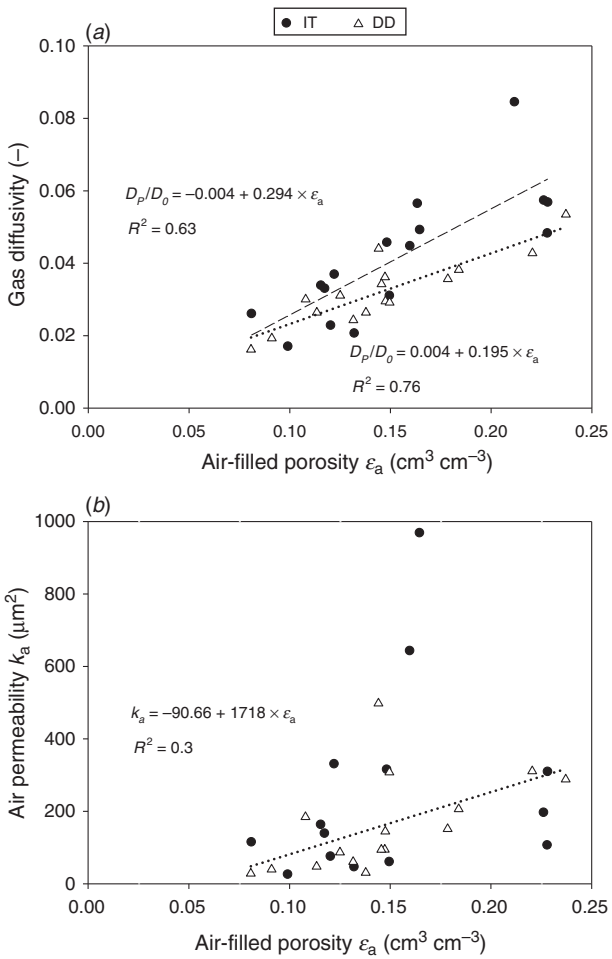

Fig. 5. Relationship between (*a*) gas diffusivity and air-filled porosity, and (*b*) air permeability and air-filled porosity under intensive tillage (IT) and direct drill (DD).

higher air permeability in conservation tillage than in IT. The parameters D_p/D_0 and d were not affected by any of the long-term treatments (Table 4). D_p/D_0 was linearly related to ε_a (Fig. 5*a*). The regression coefficients were 0.63 and 0.76 for the

IT and DD topsoils respectively. Regressing k_a with ε_a revealed a larger scatter of k_a compared with D_p/D_0 (Fig. 5*b*). This was particularly the case for the IT topsoils, which exhibited a non-linear relationship. The comparison of these two relationships reflects the dependence of ε_a on pore size and continuity (Ball 1981*b*).

The average *P*-parameter values for the IT and DD topsoils were 9177 and 4666 respectively. Both these values are high compared with loamy Danish soils with average *P*-parameter values of 700 (Kawamoto *et al*. 2006). The extremely high *P*-parameter values for the IT soil reflect that the IT soil was SOC-depleted as already seen in its high clay-to-SOC ratio (Fig. 1*c*). It seems that crossing the previously suggested Dexter index threshold value of 10 (Dexter *et al*. 2008) resulted in a shift to a more pipe-like soil structure with an overall more poorly connected pore network, as revealed by the visual inspection of the CT-derived images (Fig. 3), and also quantified in terms of MPD_{CCT}, CE_{CCT} and SMI_{CCT} (Table 2). In addition, in a multiple regression analysis 66% of the total variability of the *P*-parameter was explained by MPD_{CCT} ($\beta_1 = 0.8$), HWC ($\beta_2 = -1.9$) and SOC ($\beta_3 = 1.8$; $P < 0.0001$). Although the soils had similar TP_{CCT}, the functional pore-network structure was quite different between the DD and IT soil, supported by both gas transport measurements and derived structural parameters and the CT-derived parameters.

Relationships between soil quality and X-ray CT-derived structural parameters and functional structural parameters for soil gas exchange

The laboratory measurements of the structural parameters D_p/D_0 and k_a, necessary for characterising gas transport processes, were conducted at a matric potential of −100 cm. According to the capillary rise equation pores with a diameter larger than 30 µm were drained at this tension. The X-ray CT scans of the intact soil cores were acquired at a matric potential of −150 cm. The final CT image resolution was 33 µm meaning that only pores with a diameter larger than 33 µm were visible. The closeness of these two pore diameters associated with the

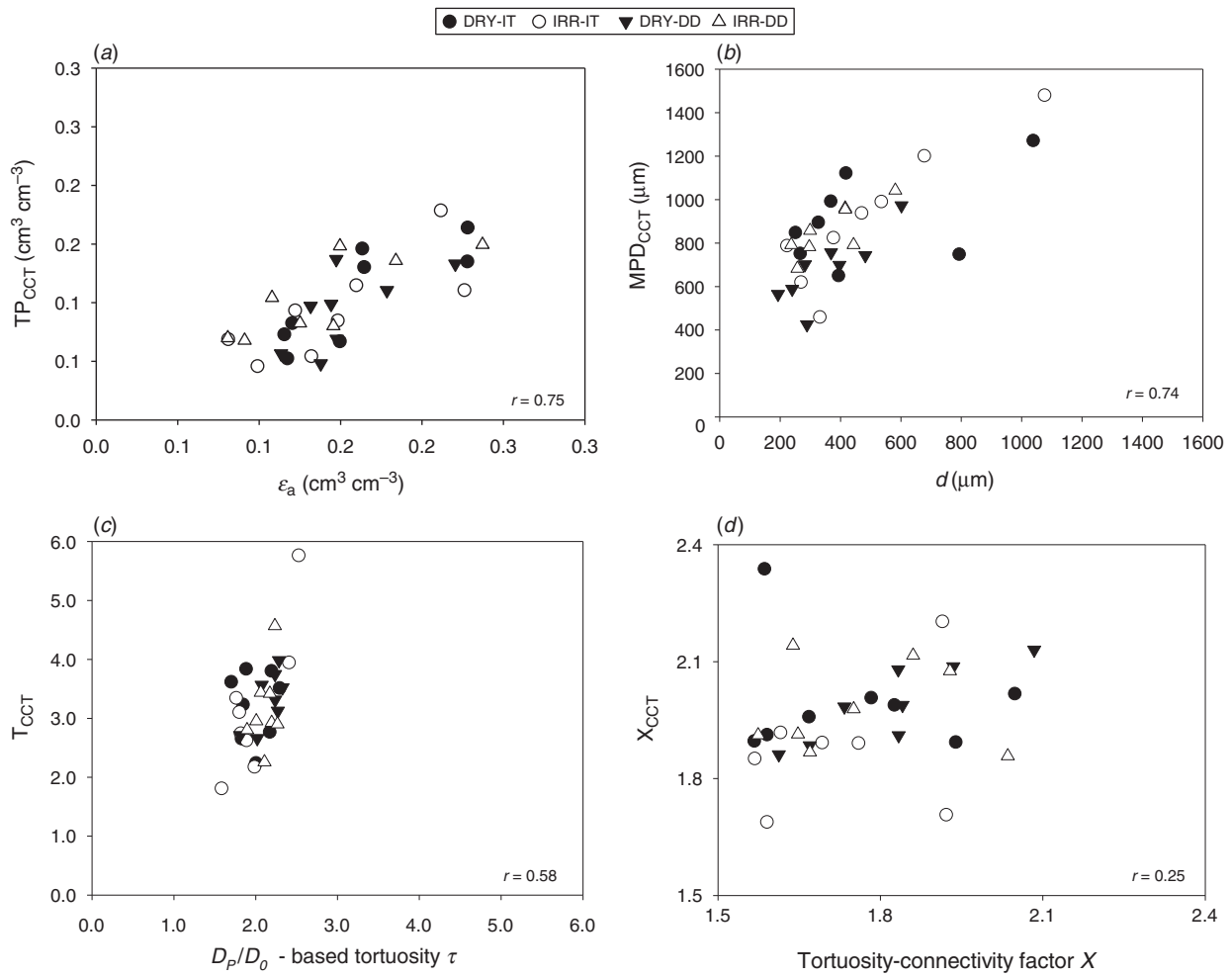

Fig. 6. Relationships between (*a*) total pore volume visible by CT and the air-filled porosity determined at −100 cm matric potential, (*b*) X-ray CT-derived mean pore diameter MPD_{CCT} and the equivalent pore diameter, *d*, (*c*) tortuosity determined from X-ray CT images and a tortuosity parameter (τ) calculated based on measurements of D_P/D_0, and (*d*) the tortuosity-connectivity factor *X* derived by X-ray CT and based on gas measurements for topsoils under different management practices (IRR, irrigated; DRY, non-irrigated; IT, intensive tillage; DD, direct drill).

Table 5. Pearson correlation coefficients (*r*) between the structural parameters derived with X-ray CT and the functional structural parameters for gas exchange processes based on gas measurements. Boldfaced figures indicate significant parameters at the 0.05 significance level

TP, total porosity; $TP_{CCT,}$ connected total porosity measured with X-ray CT; DA_{CCT}, degree of anisotropy; CE_{CCT}, connectivity; FD_{CCT}, fractal dimension; $OSVR_{CCT}$, object surface-to-volume ratio; MPD_{CCT}, mean pore diameter; SMI_{CCT}, structure model index; T_{CCT}, tortuosity; Class 1_{CCT}, TP of pores of 33–300 µm; Class 2_{CCT}, TP of pores of 300–700 µm; Class 3_{CCT}, TP of pores of 700–1003 µm; Class 4_{CCT}, TP of pores of 1003–3000 µm; Class 5_{CCT}, TP of pores >3000 µm; ε_a, air-filled porosity; k_a, air permeability; D_P/D_0, gas diffusivity; τ, tortuosity; d, equivalent pore diameter; X, X-parameter (refer to text for more information)

	ε_a	D_P/D_0	k_a	τ	d	P-parameter	X
TP	**0.80**	**0.55**	0.27	0.10	0.34	0.28	**0.65**
TP_{CCT}	**0.75**	**0.78**	**0.58**	−0.33	**0.63**	**0.59**	0.3
$OSVR_{CCT}$	−0.03	−0.24	**−0.41**	0.33	**−0.56**	**−0.49**	0.23
SMI_{CCT}	0.02	**0.41**	**0.55**	**−0.49**	0.34	**0.46**	**−0.39**
MPD_{CCT}	0.23	**0.55**	**0.70**	**−0.49**	**0.74**	**0.72**	−0.23
FD_{CCT}	**0.73**	**0.51**	0.19	0.00	0.25	0.20	**0.55**
DA_{CCT}	0.27	−0.01	−0.18	0.28	−0.14	−0.16	**0.43**
CE_{CCT}	**−0.46**	−0.33	−0.06	−0.02	0.03	0.01	**−0.35**
T_{CCT}	**−0.57**	**−0.72**	**−0.39**	**0.58**	**−0.45**	**−0.37**	−0.02
X_{CCT}	−0.09	−0.33	−0.1	**0.43**	0.01	0.03	**0.235**
Class 1_{CCT}	**0.50**	**0.36**	0.04	−0.01	−0.02	−0.01	**0.37**
Class 2_{CCT}	**0.60**	**0.36**	0.04	0.00	0.18	0.11	**0.49**
Class 3_{CCT}	**0.63**	**0.59**	**0.40**	−0.27	**0.59**	**0.48**	0.29
Class 4_{CCT}	**0.53**	**0.77**	**0.80**	**−0.48**	**0.82**	**0.80**	0.00
Class 5_{CCT}	**0.47**	**0.75**	**0.81**	**−0.44**	**0.71**	**0.75**	−0.05

measurements enabled us to relate their results, namely the soil pore architectural parameters derived from the X-ray CT images to the functional soil structural parameters D_p/D_0 and k_a. We used the CT scan parameters of the connected porosity, which were assumed to be more relevant than those derived from TP_{CT}. In addition, we investigated the relationships between soil quality and texture determined at bulk soil samples with D_p/D_0, k_a and the X-ray CT-derived structural parameters.

TP_{CCT} and ε_a were strongly correlated ($r = 0.75$) with TP_{CCT} ranging between 35 and 99% of ε_a with an average of 67% (Fig. 6*a*, Table 5) suggesting the relevance of pores between 20 and 33 µm for ε_a. Accordingly, regressing ε_a with TP_{CT} had a higher correlation coefficient ($r = 0.83$). In our topsoil, D_p/D_0 was mainly dependent on TP_{CCT} ($r = 0.78$), BD ($r = -0.79$), and tortuosity, T_{CCT} ($r = -0.72$). Higher BD reduces ε_a, leading to a subsequent reduction in D_p/D_0 at the same soil water potential. Other less strong but equally significant correlations were found with the structural parameters MPD_{CCT} ($r = 0.55$), FD_{CCT} ($r = 0.51$) and SMI_{CCT} ($r = 0.41$), highlighting pore shape and structure complexity as pivotal soil properties that affect gas transport parameters. The roughness and complexity of pores reduced gas interchange, whereas the more cylindrical and self-similar ones favoured gas diffusion. Bulk density and soil texture were identified as governing factors for D_p/D_0 (Grable and Siemer 1968), but others have found no influence of these on D_p/D_0 (Eden *et al*. 2011). The d ranged from 193 to 1076 µm and averaged 425 µm. It was significantly ($P < 0.0001$) and positively ($r = 0.74$) correlated with the mean pore diameter MPD_{CCT} determined by X-ray CT, which ranged from 425 to 1481 µm with an average of 841 µm (Fig. 6*b*). The pore classes enclosing pores from 700 to 3000 µm were equally correlated with d. It appears that MPD_{CCT} derived from CT-images could potentially be used as independently obtained parameter for predicting k_a in arable soils. Moreover, we found a positive and significant ($P < 0.001$) relationship between the tortuosity derived from the X-ray CT images T_{CCT} and the tortuosity calculated using the gas parameters determined at a matric potential of −100 cm, D_p/D_0 and ε_a, with a Pearson correlation coefficient of 0.58 (Table 5). The CT-derived tortuosity ranged between 1.81 and 5.77 and was in all cases higher than the D_p/D_0-based tortuosity, which ranged from 1.62 to 2.58 (Fig. 6*c*). In contrast, Katuwal *et al*. (2015) found consistently higher D_p/D_0-based tortuosity than CT-derived tortuosity. In their study, however, the soils were repacked, and with the exception of one soil, had lower clay (157–197 g kg^{-1}) and SOC (0.9–2%) contents than the topsoil used in our study. A less well aggregated soil structure thus can be assumed. The D_p/D_0-based tortuosity-connectivity parameter, X, ranged between 1.45 and 2.08, which is in the range of values reported by others (e.g. Chamindu Deepagoda *et al*. 2012). The X_{CCT} maximum value was 2.34 and the minimum value was 1.69. But although the range was rather similar to X, the correlation between the two parameters was relatively weak ($r = 0.25$) (Table 5; Fig. 6*d*). The variation of the parameter is small but not negligible as commonly assumed in D_p/D_0 power function models and recently discussed by Katuwal *et al*. (2015).

Conclusions

In this study we analysed the effect of long-term agricultural intensification defined as irrigation and IT on soil quality and structural parameters. Irrigation had no significant effect on any of the parameters measured. In contrast, IT increased the Dexter index of the topsoil, which resulted in higher BD and lower TP. The Dexter index crossed the previously proposed critical threshold of 10 resulting in a more pipe-like soil structure with an overall more poorly connected pore network under IT compared with DD. This was also reflected by the CT-derived structural parameters MPD_{CCT}, CE_{CCT} and SMI_{CCT} and the functional pore-structural P-parameter. Differences in pore morphometrical parameters such as P-parameter, pore size distribution and pore shape were attributed to mechanical disturbance and SOC depletion through IT. Moreover, significant correlations between structural parameters derived with X-ray CT and air permeability and gas diffusivity measurements verified that X-ray CT parameters might be useful proxies for relevant functional parameters including equivalent pore diameter, connectivity and tortuosity required to predict gas diffusivity and air permeability. This is a first step to test this concept on soil collected as intact cores from a site under long-term arable production.

Conflicts of interest

The authors declare no conflicts of interest.

Acknowledgements

This project was funded through the New Zealand Ministry for Business Innovation and Education (Contract 34573) and the European-RISE project 'PROTINUS' (Contract 645717) with counter-funding from the Royal Society of New Zealand. Thanks are due to Paul Mudge and Bryan Stevenson for discussions around the study design and site selection, FAR for granting us access to their property, Andre, Matteo, Kathryn, Stephanie, Frank and Bodil for assistance with laboratory and field work.

References

Al-Kaisi MM, Yin X, Licht MA (2005) Soil carbon and nitrogen changes as influenced by tillage and cropping systems in some Iowa soils. *Agriculture, Ecosystems & Environment* **105**, 635–647. doi:10.1016/j.agee.2004.08.002

Arganda-Carreras I, Kaynig V, Rueden C, Eliceiri KW, Schindelin J, Cardona A, Sebastian Seung H (2017) Trainable Weka Segmentation: a machine learning tool for microscopy pixel classification. *Bioinformatics* **33**, 2424–2426. doi:10.1093/bioinformatics/btx180

Badalıkova B (2010) Influence of soil tillage on soil compaction. In 'Soil engineering'. (Eds AP Dedousis, T Bartzanas) pp. 19–30. (Springer-Verlag: Berlin Heidelberg) doi:doi:10.1007/978-3-642-03681-1_2

Baker JM, Ochsner TE, Venterea RT, Griffis TJ (2007) Tillage and soil carbon sequestration – What do we really know? *Agriculture, Ecosystems & Environment* **118**, 1–5. doi:10.1016/j.agee.2006.05.014

Ball BC (1981*a*) Modelling of soil pores as tubes using gas permeabilities, gas diffusivities and water release. *Journal of Soil Science* **32**, 465–481. doi:10.1111/j.1365-2389.1981.tb01723.x

Ball BC (1981*b*) Pore characteristics of soils from two cultivation experiments as shown by gas diffusivities and permeabilities and air-filled porosities. *Journal of Soil Science* **32**, 483–498. doi:10.1111/j.1365-2389.1981.tb01724.x

Ball BC (2013) Soil structure and greenhouse gas emissions: a synthesis of 20 years of experimentation. *European Journal of Soil Science* **64**, 357–373. doi:10.1111/ejss.12013

Blakemore L, Searle PL, Daly BK (1987) Methods for chemical analysis of soils. pp. 103. New Zealand Soil Bureau Scientific Report 80: Lower Hutt, NZ.

Chamindu Deepagoda TKK, Moldrup P, Schjønning P, Kawamoto K, Komatsu T, de Jonge LW (2012) Variable pore connectivity model linking gas diffusivity and air-phase tortuosity to soil matric potential. *Vadose Zone Journal* **11**. doi:10.2136/vzj2011.0096

Chatterjee S, Bandyopadhyay KK, Pradhan S, Singh R, Datta SP (2018) Effects of irrigation, crop residue mulch and nitrogen management in maize (*Zea mays* L.) on soil carbon pools in a sandy loam soil of Indo-gangetic plain region. *Catena* **165**, 207–216. doi:10.1016/j.catena.2018.02.005

D'Haene K, Vermang J, Cornelis WM, Leroy BLM, Schiettecatte W, De Neve S, Gabriels D, Hofman G (2008) Reduced tillage effects on physical properties of silt loam soils growing root crops. *Soil & Tillage Research* **99**, 279–290. doi:10.1016/j.still.2008.03.003

Dal Ferro N, Sartori L, Simonetti G, Berti A, Morari F (2014) Soil macro- and microstructure as affected by different tillage systems and their effects on maize root growth. *Soil & Tillage Research* **140**, 55–65. doi:10.1016/j.still.2014.02.003

Deen W, Kataki PK (2003) Carbon sequestration in a long-term conventional versus conservation tillage experiment. *Soil & Tillage Research* **74**, 143–150. doi:10.1016/S0167-1987(03)00162-4

Deng Y, Cai C, Xia D, Ding S, Chen J (2017) Fractal features of soil particle size distribution under different land-use patterns in the alluvial fans of collapsing gullies in the hilly granitic region of southern China. *PLoS One* **12**, e0173555. doi:10.1371/journal.pone.0173555

Dersch G, Bohm K (2001) Effects of agronomic practices on the soil carbon storage potential in arable farming in Austria. *Nutrient Cycling in Agroecosystems* **60**, 49–55. doi:10.1023/A:1012607112247

Dexter AR (2004) Soil physical quality: Part I. Theory, effects of soil texture, density, and organic matter, and effects on root growth. *Geoderma* **120**, 201–214. doi:10.1016/j.geoderma.2003.09.004

Dexter AR, Richard G, Arrouays D, Czyż EA, Jolivet C, Duval O (2008) Complexed organic matter controls soil physical properties. *Geoderma* **144**, 620–627. doi:10.1016/j.geoderma.2008.01.022

Dick WA (1983) Organic carbon, nitrogen, and phosphorus concentrations and pH in soil profiles as affected by tillage intensity. *Soil Science Society of America Journal* **47**, 102–107. doi:10.2136/sssaj1983.03615995004700010021x

Eden M, Schjønning P, Moldrup P, de Jonge LW (2011) Compaction and rotovation effects on soil pore characteristics of a loamy sand soil with contrasting organic matter content. *Soil Use and Management* **27**, 340–349. doi:10.1111/j.1475-2743.2011.00344.x

Entry JA, Sojka RE, Shewmaker GE (2004) Irrigation increases inorganic carbon in agricultural soils. *Environmental Management* **33**(Suppl), S309–S317. doi:10.1007/s00267-003-9140-3

FAO (2006) World reference base for soil resources. FAO, No. World Soil Resources Reports No. 103, Rome.

Fish AN, Koppi AJ (1994) The use of a simple field air permeameter as a rapid indicator of functional soil pore space. *Geoderma* **63**, 255–264. doi:10.1016/0016-7061(94)90067-1

Garbout A, Munkholm LJ, Hansen SB (2013) Tillage effects on topsoil structural quality assessed using X-ray CT, soil cores and visual soil evaluation. *Soil & Tillage Research* **128**, 104–109. doi:10.1016/j.still.2012.11.003

Ghani A, Dexter M, Perrott KW (2003) Hot-water extractable carbon in soils: a sensitive measurement for determining impacts of fertilisation, grazing and cultivation. *Soil Biology & Biochemistry* **35**, 1231–1243. doi:10.1016/S0038-0717(03)00186-X

González-Sánchez EJ, Ordóñez-Fernández R, Carbonell-Bojollo R, Veroz-González O, Gil-Ribes JA (2012) Meta-analysis on atmospheric carbon capture in Spain through the use of conservation agriculture. *Soil & Tillage Research* **122**, 52–60. doi:10.1016/j.still.2012.03.001

Grable AR, Siemer EG (1968) Effect of bulk density, aggregate size, and soil water suction on oxygen diffusion, redox potentials, and elongation of corn roots. *Soil Science Society of America Journal* **32**, 180–186. doi:10.2136/sssaj1968.03615995003200020011x

Harrigan TP, Mann RW (1984) Characterization of microstructural anisotropy in orthotropic materials using a second rank tensor. *Journal of Materials Science* **19**, 761–767. doi:10.1007/BF00540446

Havlin JL, Kissel DE, Maddux LD, Claassen MM, Long JH (1990) Crop rotation and tillage effects on soil organic carbon and nitrogen. *Soil Science Society of America Journal* **54**, 448–452. doi:10.2136/sssaj1990.03615995005400020026x

Hewitt AE (2010) 'New Zealand soil classification', 3rd edn. Landcare Research Science Series No. 1. (Manaaki Whenua Press: Lincoln).

Hildebrand TOR, Rügsegger P (1997) Quantification of bone microarchitecture with the structure model index. *Computer Methods in Biomechanics and Biomedical Engineering* **1**, 15–23. doi:10.1080/01495739708936692

Katuwal S, Arthur E, Tuller M, Moldrup P, de Jonge LW (2015) Quantification of soil pore network complexity with X-ray computed tomography and gas transport measurements. *Soil Science Society of America Journal* **79**, 1577–1589. doi:10.2136/sssaj2015.06.0227

Kawamoto K, Moldrup P, Schjønning P, Iversen BV, Komatsu T, Rolston DE (2006) Gas transport parameters in the vadose zone: development

and tests of power-law models for air permeability. *Vadose Zone Journal* **5**, 1205–1215. doi:10.2136/vzj2006.0030

Kay BD, Vanden Bygaart AJ (2002) Conservation tillage and depth stratification of porosity and soil organic matter. *Soil & Tillage Research* **66**, 107–118. doi:10.1016/S0167-1987(02)00019-3

Khademzadeh S, Carmignato S, Parvin N, Zanini F, Bariani PF (2016) Micro porosity analysis in additive manufactured NiTi parts using micro computed tomography and electron microscopy. *Materials and Design* **90**, 745–752. doi:10.1016/j.matdes.2015.10.161

Ludwig B, Geisseler D, Michel K, Joergensen RG, Schulz E, Merbach I, Raupp J, Rauber R, Hu K, Niu L, Liu X (2011) Effects of fertilization and soil management on crop yields and carbon stabilization in soils. A review. *Agronomy for Sustainable Development* **31**, 361–372. doi:10.1051/agro/2010030

Moldrup P, Poulsen TG, Schjønning P, Olesen T, Yamaguchi T (1998) Gas permeability in undisturbed soils: measurements and predictive models. *Soil Science* **163**, 180–189. doi:10.1097/00010694-199803000-00002

Moldrup P, Olesen T, Komatsu T, Schjønning P, Rolston DE (2001) Tortuosity, diffusivity, and permeability in the soil liquid and gaseous phases. *Soil Science Society of America Journal* **65**, 613–623. doi:10.2136/sssaj2001.653613x

Mudge PL, Kelliher FM, Knight TL, O'Connell D, Fraser S, Schipper LA (2017) Irrigating grazed pasture decreases soil carbon and nitrogen stocks. *Global Change Biology* **23**, 945–954. doi:10.1111/gcb.13448

Munkholm LJ, Heck RJ, Deen B (2013) Long-term rotation and tillage effects on soil structure and crop yield. *Soil & Tillage Research* **127**, 85–91. doi:10.1016/j.still.2012.02.007

Naveed M, Hamamoto S, Kawamoto K, Sakaki T, Takahashi M, Komatsu T, Moldrup P, Lamandé M, Wildenschild D, Prodanovic M, de Jonge LW (2013) Correlating gas transport parameters and X-ray computed tomography measurements in porous media. *Soil Science* **178**, 60–68. doi:10.1097/SS.0b013e318288784c

Pagliai M, Vignozzi N, Pellegrini S (2004) Soil structure and the effect of management practices. *Soil & Tillage Research* **79**, 131–143. doi:10.1016/j.still.2004.07.002

Papadopoulos A, Bird NRA, Whitmore AP, Mooney SJ (2009) Investigating the effects of organic and conventional management on soil aggregate stability using X-ray computed tomography. *European Journal of Soil Science* **60**, 360–368. doi:10.1111/j.1365-2389.2009.01126.x

Pareja-Sánchez E, Plaza-Bonilla D, Ramos MC, Lampurlanés J, Álvaro-Fuentes J, Cantero-Martínez C (2017) Long-term no-till as a means to maintain soil surface structure in an agroecosystem transformed into irrigation. *Soil & Tillage Research* **174**, 221–230. doi:10.1016/j.still.2017.07.012

Perret JS, Prasher SO, Kacimov AR (2003) Mass fractal dimension of soil macropores using computed tomography: from the box-counting to the cube-counting algorithm. *European Journal of Soil Science* **54**, 569–579. doi:10.1046/j.1365-2389.2003.00546.x

Piccoli I, Camarotto C, Lazzaro B, Furlan L, Morari F (2017*a*) Conservation agriculture had a poor impact on the soil porosity of Veneto Low-lying Plain silty soils after a 5-year transition period. *Land Degradation & Development* **28**, 2039–2050. doi:10.1002/ldr.2726

Piccoli I, Schjønning P, Lamandé M, Furlan L, Morari F (2017*b*) Challenges of conservation agriculture practices on silty soils. Effects on soil pore and gas transport characteristics in North-eastern Italy. *Soil & Tillage Research* **172**, 12–21. doi:10.1016/j.still.2017.05.002

Pires LF, Borges JAR, Rosa JA, Cooper M, Heck RJ, Passoni S, Roque WL (2017) Soil structure changes induced by tillage systems. *Soil & Tillage Research* **165**, 66–79. doi:10.1016/j.still.2016.07.010

Powlson DS, Stirling CM, Jat ML, Gerard BG, Palm CA, Sanchez PA, Cassman KG (2014) Limited potential of no-till agriculture for climate change mitigation. *Nature Climate Change* **4**, 678–683. doi:10.1038/nclimate2292

Puget P, Lal R (2005) Soil organic carbon and nitrogen in a Mollisol in central Ohio as affected by tillage and land use. *Soil & Tillage Research* **80**, 201–213. doi:10.1016/j.still.2004.03.018

Rolston DE, Moldrup P (2002) 4.3 Gas diffusivity. In 'Methods of soil analysis: part 4 physical methods'. (Eds JH Dane, CG Topp) pp. 1113–1139. (Soil Science Society of America: Madison, WI)

Schjønning P, Koppelgaard M (2017) The Forchheimer approach for soil air permeability measurement. *Soil Science Society of America Journal* **81**, 1045–1053. doi:10.2136/sssaj2017.02.0056

Schjønning P, Eden M, Moldrup P, de Jonge LW (2013) Two-chamber, two-gas and one-chamber, one-gas methods for measuring the soil-gas diffusion coefficient: validation and inter-calibration. *Soil Science Society of America Journal* **77**, 729–740. doi:10.2136/sssaj2012.0379

Schlüter S, Weller U, Vogel HJ (2011) Soil-structure development including seasonal dynamics in a long-term fertilization experiment. *Journal of Plant Nutrition and Soil Science* **174**, 395–403. doi:10.1002/jpln.201000103

Scott JT, Stewart DPC, Metherell AK (2012) Alteration of pasture root carbon turnover in response to superphosphate and irrigation at Winchmore New Zealand. *New Zealand Journal of Agricultural Research* **55**, 147–159. doi:10.1080/00288233.2012.662896

Siebert S, Döll P (2010) Quantifying blue and green virtual water contents in global crop production as well as potential production losses without irrigation. *Journal of Hydrology* **384**, 198–217. doi:10.1016/j.jhydrol.2009.07.031

Soane B, Ball B (1998) Review of management and conduct of long-term tillage studies with special reference to a 25-yr experiment on barley in Scotland. *Soil & Tillage Research* **45**, 17–37. doi:10.1016/S0167-1987(97)00070-6

Tebrügge F, Düring RA (1999) Reducing tillage intensity — a review of results from a long-term study in Germany. *Soil & Tillage Research* **53**, 15–28. doi:10.1016/S0167-1987(99)00073-2

Trost B, Prochnow A, Drastig K, Meyer-Aurich A, Ellmer F, Baumecker M (2013) Irrigation, soil organic carbon and N_2O emissions. A review. *Agronomy for Sustainable Development* **33**, 733–749. doi:10.1007/s13593-013-0134-0

Ulrich D, van Rietbergen B, Laib A, Ruegsegger P (1999) The ability of three-dimensional structural indices to reflect mechanical aspects of trabecular bone. *Bone* **25**, 55–60. doi:10.1016/S8756-3282(99)00098-8

Verheye W, Ameryckx J (1984) Mineral fractions and classification of soil texture. *Pédologie (Gent)* **34**, 215–225.

Vogel HJ (1997) Morphological determination of pore connectivity as a function of pore size using serial sections. *European Journal of Soil Science* **48**, 365–377. doi:10.1046/j.1365-2389.1997.00096.x

Vogeler I, Rogasik J, Funder U, Panten K, Schnug E (2009) Effect of tillage systems and P-fertilization on soil physical and chemical properties, crop yield and nutrient uptake. *Soil & Tillage Research* **103**, 137–143. doi:10.1016/j.still.2008.10.004

Wahl NA, Bens O, Buczko U, Hangen E, Hüttl RF (2004) Effects of conventional and conservation tillage on soil hydraulic properties of a silty-loamy soil. *Physics and Chemistry of the Earth Parts A/B/C* **29**, 821–829. doi:10.1016/j.pce.2004.05.009

Yang X-M, Wander MM (1999) Tillage effects on soil organic carbon distribution and storage in a silt loam soil in Illinois. *Soil & Tillage Research* **52**, 1–9. doi:10.1016/S0167-1987(99)00051-3

Zanini F, Carmignato S (2017) Two-spheres method for evaluating the metrological structural resolution in dimensional computed tomography. *Measurement Science and Technology* **28**, 114002. doi:10.1088/1361-6501/aa85b7

Handling editor: Celine Duwig